Novel Load Following Controller of Microturbine Generation System for Stand-Alone/Grid-Connected Operation

Pouyan Asgharian[1*], Reza Noroozian[2]
1- Department of Electrical Engineering, Faculty of Engineering, University of Zanjan, Zanjan, Iran.
Email: pouyan.asgharian@znu.ac.ir (Corresponding author)
2- Department of Electrical Engineering, Faculty of Engineering, University of Zanjan, Zanjan, Iran.
Email: noroozian@znu.ac.ir

Received: September 2018 Revised: November 2018 Accepted: February 2019

ABSTRACT:
Among various types of Distributed Generations, Microturbine (MT) Generation (MTG) systems are known as highly reliable and efficient sources. The MT must support demands in different conditions, which requires its proper control. In this paper, hybrid operation of the MTG is considered which is initially isolated from utility grid, and after that it is connected to the distribution network. A robust control method is used for stand-alone mode and a novel power-voltage control strategy is applied to grid-tied inverter. In stand-alone mode, the voltage, frequency and current are used as control parameters instead of traditional voltage-frequency control. In grid-connected novel controller, the inner voltage loop is substituted with the current loop, so it is based on powers and voltage. The simulations are performed by MATLAB/Simulink, with the results indicating proper power sharing as well as load-following performance with the minimum level of distortion. The proposed strategy can be used in hybrid operations of the MTG.

KEYWORDS: Microturbine, Stand-Alone Mode, Grid-Connected Mode, Load-Following Performance, Flexible Operation.

1. INTRODUCTION

Over the past decade, researches have been trying to analyze various types of Distributed Generations (DG) such as wind turbine, photovoltaic, microturbine, and fuel cell in grid-connected or stand-alone modes. It is widely accepted that MTG system is one of the most suitable means in this area.

Because of the MTs inherent characteristics, they are used in a variety of, sometimes challenging applications [1]. The MT should follow load variations to properly supply demands, so load-following performance is a major issue [2].

The MTG dynamic modeling and its performance analysis in stand-alone or grid-connected modes are solved problems [3-7]. New methods in this area have helped the MTG to operate properly. For example, modeling and controlling the MT based GAST model with active power is a suitable method [8] for connecting to network.

Simultaneous performance (grid-connected/stand-alone) of the MTG with a novel passive filter called Remover Ripple Circuit (RRC) has been presented in [9] as a new MTG operational aspect. The dynamic modeling and comprehensive load-following performance analysis of a split-shaft MT have been illustrated in [10].

Use of algorithms and control methods can be useful. Detailed dynamic modeling and controlling based on Model Predictive Control (MPC) [11] and differential evolutionary algorithm [12] have been presented to improve the MTG performance.

Hybrid energy systems (especially renewable generation) with the MTG [13-16] are an efficient strategy to generate highly reliable power for consumers. The erratic nature of renewable energies requires a quick and highly reliable source.

In the mentioned papers, the MTG stand-alone or grid-connected modes have been investigated for various operational conditions, but hybrid operation mode has not been considered. Also, the MTG control methods involve almost traditional voltage-frequency for stand-alone mode and power-current for grid-connected mode.

The purpose of this paper is to examine the MT hybrid operation with a different and novel control method. The MT should have high flexibility in supplying loads, and it must change the current state quickly for new positions. In other words, the control strategy plays an important role in this area.

A robust voltage-frequency control method is used for stand-alone mode, whereas when the MTG is connected to distribution network, a power-voltage

method is applied. In addition, this strategy offers superior advantages to the traditional power-current method in weak grids. The proposed strategies will lead to a new aspect of the MTG performance analysis.

The simulation results confirm load-following performance and quick response of the MTG. These control methods can be used in hybrid operations, stand-alone with load variations or simultaneous operations.

The rest of this paper is organized as follows: Section 2 briefly explains the MTG system, Sections 3 and 4 are dedicated to MTG modeling and control configuration for stand-alone/grid-connected modes, respectively. Finally, the simulation results and conclusion are presented in Sections 5 and 6, respectively.

2. MICROTURBINE SYSTEM

MTs are indeed small gas turbines operating based on the Brayton thermodynamic cycle [3]. Their output power ranges from 25 kW to 1 MW and their efficiency is about 20-30%; however, an efficiency of over 80% will be possible with Combined Heat and Power (CHP) [1, 3].

Generally, MTGs offer advantages including compact size, low initial and maintenance cost, high reliability, control simplicity, and low emission level as well as the potential of operation with various fuels such as natural gas, diesel, propane, kerosene, and biogas [3, 9]. Due to the mentioned advantages and potential merits of MTs, they can be used in many applications including peak shaving, base load, and transportation systems [1, 3].

MT's production system is similar to that of gas turbine. The main components include compressor, combustion chamber, turbine, recuperator, and Permanent Magnet Synchronous Generator (PMSG) [11].

First, the fresh air is drawn in to a compressor, which increases the air pressure. Afterwards, the compressed air mixes with fuel (e.g. natural gas) to raise its temperature and pressure. Then, the hot air expands through a turbine, which eventually makes PMSG rotate fast, thereby providing electric power.

The recuperator is employed to increase the efficiency of this cycle [9]. Recuperator is actually a heat exchanger which transfers heat from output hot gases to the compressed air, resulting in less fuel consumption [4].

There are two types of MTs based on how the above equipment is mounted, namely single-shaft and split-shaft [3]. In the case of single-shaft, all equipment is mounted on a shaft and due to the very high rotation speed, the output frequency is about 1-4 kHz. In the split-shaft model, however, there are two turbines and two separate parts which are connected through a gear. The output frequency is about 50-60 Hz and there is no need for power electronic interface [11].

Single-shaft MT is more common owing to its less maintenance and lubrication requirements. Typically, due to their simplicity and low cost, AC-DC-AC power electronic converters are employed, which first convert the high frequency voltage to the DC voltage using rectifier and then convert it back again to the desired AC voltage (50 or 60 Hz) with the desired frequency and domain using an inverter. These types of converters are called double conversion systems.

Fig. 1 demonstrates AC-DC-AC based single-shaft MT for two different operational modes. The power flow of this system is illustrated in Fig. 2.

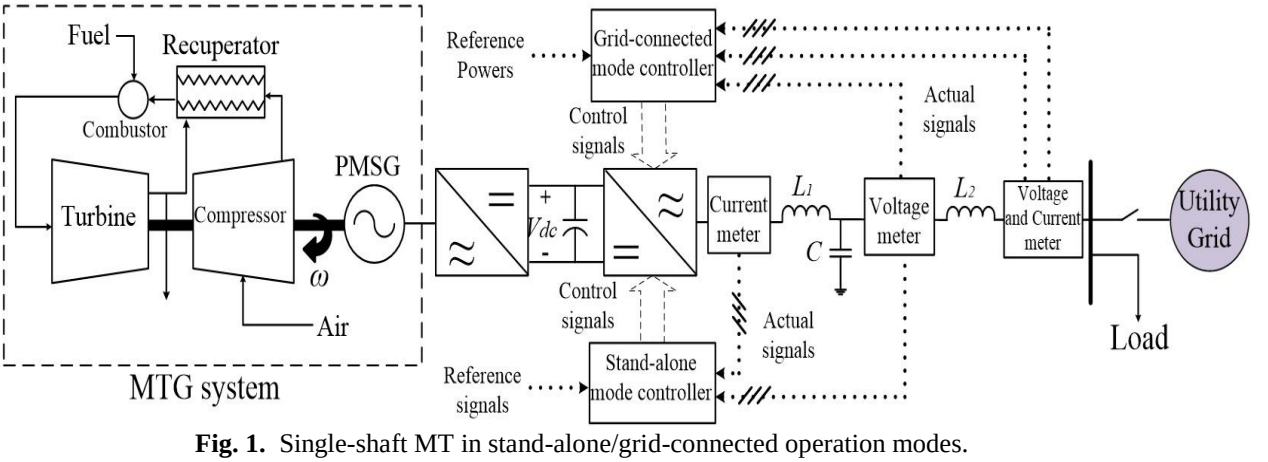

Fig. 1. Single-shaft MT in stand-alone/grid-connected operation modes.

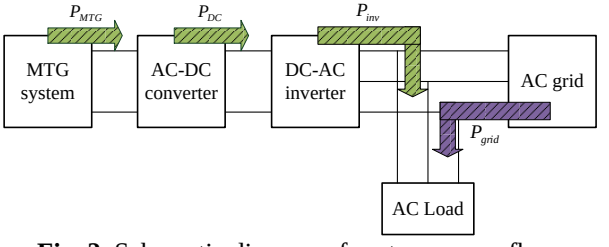

Fig. 2. Schematic diagram of system power flow.

3. MICROTURBINE GENERATION SYSTEM MODELING

3.1. MT Modeling

As mentioned previously, the single-shaft MT consists of compressor, combustor, turbine, PMSG and recuperator in the format of five controller parts. Dynamic model of an MT is shown in Fig. 3 including speed control, acceleration control, fuel system, temperature control and turbine dynamics.

Speed control operates based on error between reference speed (1 per unit) and rotor speed. A lead-lag transfer function or Proportional-Integral-Derivative (PID) controller is used to model speed governor [4]. In this paper, a lead-lag transfer function with constant values is considered.

$$Gov = (25 \times \frac{0.4s+1}{0.05s+1}) \times (1 - W_m) \quad (1)$$

Where *Gov* is speed controller output, W_m is PMSG rotor speed. Acceleration control is used to limit increase of rate of rotor speed at start-up of the MT. This block can be ignored when the rotor speed is near the rated speed [9].

Control of turbine exhaust at a predetermined firing temperature is done by temperature control. Temperature control consists of thermocouple and radiation shield series blocks. The output of thermocouple is compared with reference temperature (950 °F). When the thermocouple output exceeds the reference temperature, a negative difference cause to reduce temperature [3]. The exhaust temperature characteristic is as follows:

$$f_1 = 950 + 550(1 - W_m) - 700(1 - W_f) \quad (2)$$

Where, W_f is fuel system output (after time delays). Outputs of the speed governor, acceleration control and temperature control are entered to Min block to achieve the least value. Output signal (V_{CE}) is passed through a limiter to enter to fuel system. Limiter has an important role to maintain fuel demand as well as fire in a desirable condition. V_{CE} is scaled by 0.77 and offset by 0.23 that represents fuel flow at no load condition. Gas turbine requires 23% fuel at no load condition and this is a major deficiency of them [3].

Fuel system consists of two series blocks which are valve positioner and actuator. There are two times of delay after fuel system. One is corresponding to combustor delay and another relates to flow transferring.

Finally, burnet fuel is entered to turbine to produce mechanical power. Compressor and turbine are considered as a package because they are coupled together. The turbine dynamic is modeled by following transfer function:

$$f_2 = 1.3(W_t - 0.23) + 0.5(1 - W_m) \quad (3)$$

Where, W_t is turbine dynamic output. Therefore, in general, the PMSG rotational speed is input of the

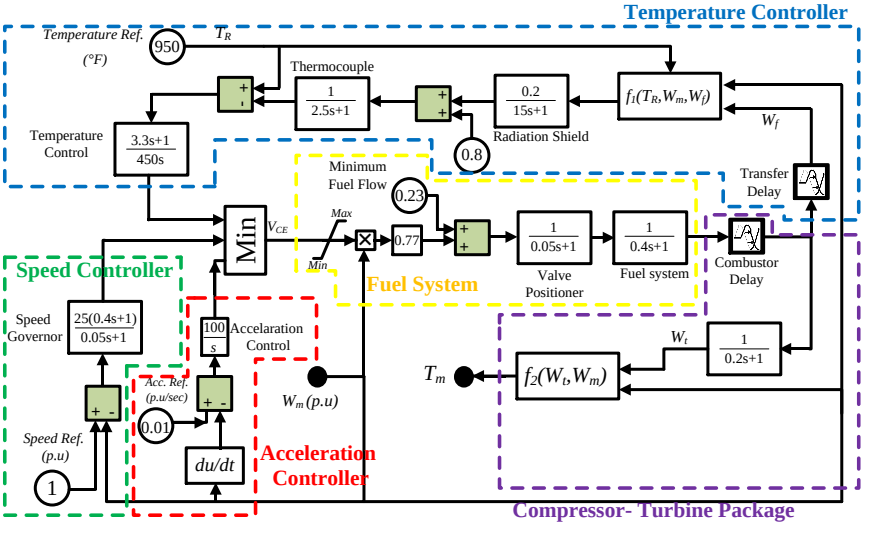

Fig. 3. The MT dynamic model.

system and mechanical torque is the output. Note that, all controllers operate in Per Unit (P. U.) except temperature control. The recuperator is not considered in the model because it is a heat exchanger to increase efficiency and it has long time constant along with little influence on dynamic behavior.

3.2. PMSG Modeling

The PSMG is a subset of synchronous generator in which rotor winding is replaced by permanent magnet. It is used instead of typical synchronous generator because of rotor lower power losses, lower maintenance costs, higher reliability, flexible configuration and it does not require to separate excitation system [17].

In this paper, a two-pole generator with a non-salient rotor at 1600 Hz (96,000 rpm) is considered. The machine output power is 30 kW and its terminal line-to-line voltage is 480 V. other parameters are: L_d=L_q=0.6875 mH, r_s=0.2503 Ω. It is assumed that flux established by the permanent magnet is sinusoidal, which caused sinusoidal electromotive forces [9]. Electrical and mechanical equations (in *dq* frame) for a two pole Permanent Magnet Synchronous Motor (PMSM) are as follows:

- Electrical equations:

$$v_d = r_s i_d + L_d \frac{di_d}{dt} - \omega_m L_q i_q \quad (4)$$

$$v_q = r_s i_q + L_q \frac{di_q}{dt} + \omega_m L_d i_d + \lambda_f \omega_m \quad (5)$$

$$T_e = \frac{3}{2}\left[\lambda_f i_q + (L_d - L_q) i_q i_d\right] \quad (6)$$

Where, L_d and L_q are *d* and *q* axis inductances, respectively, r_s is stator winding resistance, i_d and i_q are *d* and *q* axis currents, respectively, v_d and v_q are *d* and *q* axis voltages, respectively, ω_m (=W_m) is mechanical angular velocity, λ_f is flux linkage and T_e is electromagnetic torque.

- Mechanical equations:

$$\frac{d\theta_m}{dt} = \omega_m \quad (7)$$

$$\frac{d\omega_m}{dt} = \frac{1}{J}\left(T_e - T_m - F\omega_m\right) \quad (8)$$

Where, *J* is rotor and load inertia, *F* is rotor and load combined viscous friction, T_m is mechanical torque and θ_m is rotor angular position.

According to mentioned equations, equivalent circuit of the PMSG is shown in Fig. 4. Note that, mentioned equations are related to PMSM and reverse current direction along with negative electric torque are correspond to PMSG [3].

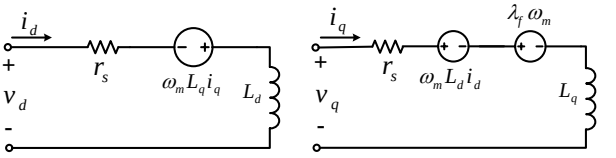

Fig. 4. PMSM equivalent circuit model: a) *d*-axis, b) *q*-axis.

4. CONTROL CONFIGURATION

In this paper, AC-DC-AC structure based on uncontrolled rectifier is considered where only the inverter is controllable. The MT high frequency output converts to DC voltage and then through an inverter it converts back to AC desirable amplitude and frequency. The inverter is connected to a load or distribution network. The purpose of parallel operation with grid includes achieving higher reliability, peak shaving, and grid support [7].

4.1. Isolated Inverter

When the inverter operates in a stand-alone mode, the voltage and frequency regulation is important [18]. Fig. 5 shows the isolated inverter control scheme. The measured voltages and currents are compared with reference values and then they are regulated by Proportional-Integral (PI) controllers. The frequency is obtained through a Phase Locked Loop (PLL).

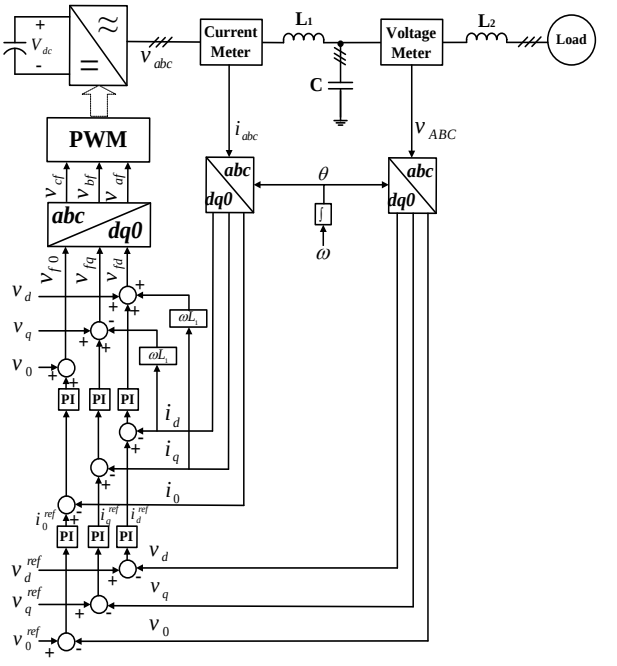

Fig. 5. Inverter control in stand-alone mode.

The following equations can be expressed for three-phase voltages and currents:

$$\begin{bmatrix} v_a \\ v_b \\ v_c \end{bmatrix} = \begin{bmatrix} v_A \\ v_B \\ v_C \end{bmatrix} + L_1 \frac{d}{dt} \begin{bmatrix} i_a \\ i_b \\ i_c \end{bmatrix} \quad (9)$$

$$i_a + i_b + i_c = 0 \quad (10)$$

Where, v_a, v_b and v_c are inverter output line-to neutral voltages, v_A, v_B and v_C are line-to-neutral capacitor voltages, L_1 is filter inductance and i_a, i_b and i_c are inverter output currents.

The control circuit consists of an inner current loop and an outer voltage loop which have independent PI controllers [18]. Initially, the measured output voltages and currents are transformed from *abc* to *dq0* frame. The voltage equation in *dq* is as follows:

$$\begin{bmatrix} v_{fd} \\ v_{fq} \\ v_{f0} \end{bmatrix} = \begin{bmatrix} v_d \\ v_q \\ v_0 \end{bmatrix} + L_1 \frac{d}{dt} \begin{bmatrix} i_d \\ i_q \\ i_0 \end{bmatrix} + \omega L_1 \begin{bmatrix} -i_q \\ i_d \\ 0 \end{bmatrix} \quad (11)$$

Where, i_d, i_q and i_0 are currents before the filter, v_{fd}, v_{fq}, v_{f0} and v_d, v_q, v_0 are voltages before and after the filter, respectively.

The reference currents in the inner control loop are obtained by voltages:

$$i_d^{ref} = PI\,(v_d^{ref} - v_d) \quad (12)$$

$$i_q^{ref} = PI\,(v_q^{ref} - v_q) \quad (13)$$

$$i_0^{ref} = PI\,(v_0^{ref} - v_0) \quad (14)$$

Finally, the output voltages from the PI controllers can be expressed as below:

$$v_{fd} = PI\,(i_d^{ref} - i_d) + v_d + \omega L_1 i_q \quad (15)$$

$$v_{fq} = PI\,(i_q^{ref} - i_q) + v_q - \omega L_1 i_d \quad (16)$$

$$v_{f0} = PI\,(i_0^{ref} - i_0) + v_0 \quad (17)$$

The control signals are obtained via inverse transformation from *dq0* to *abc*. Appropriate switching is generated through Pulse Width Modulation (PWM) block by transformed voltages v_{af}, v_{bf}, and v_{cf}. This robust control strategy generates sinusoidal waveforms with low Total Harmonic Distortion (THD).

4.2. Grid-tied Inverter

In this mode, the grid is similar to an infinite bus which imposes voltage amplitude and frequency. The configuration of the proposed power-voltage control strategy is presented in Fig. 6. The inverter has been connected to a distribution grid through a passive filter, which consists of the inverter-side inductance L_1, the grid-side inductance L_2, and filter capacitor C. the sum of transmission line inductances is represented by equivalent inductance L_g. The active power and the reactive power have been taken as control objectives [19].

This strategy employs inner voltage loop instead of the traditional current loop. The PLL is utilized to obtain voltage phase. Initially, the difference of powers is passed through PI controllers to generate reference voltages as:

$$v_q^{ref} = PI\,(P - P_{ref}) \quad (18)$$

$$v_d^{ref} = PI\,(Q - Q_{ref}) \quad (19)$$

After that, v_{fd}, v_{fq}, and v_{f0} are achieved by other PI regulators to form switching signals. The injected active

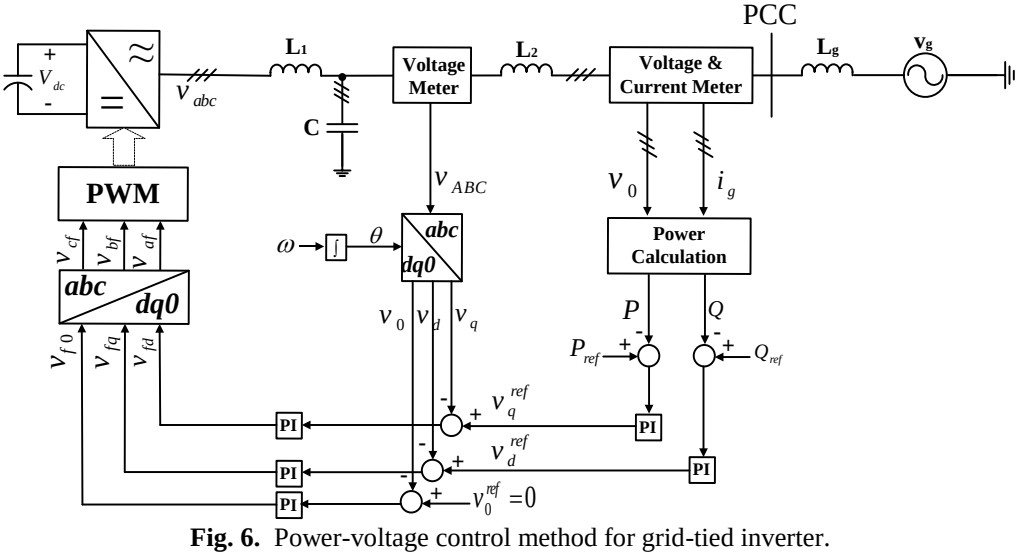

Fig. 6. Power-voltage control method for grid-tied inverter.

Table 1. Studied system parameters.

Parameter	Value
MTG output power	30 kW
MTG output frequency	1.6 kHz
MTG output voltage: V_{L-L}	480 V
DC-link voltage	760 V
DC-link capacitor	4700 µF
Filter capacitor	300 µF
Filter inductance	3 mH
Load resistance	50 Ω
Load inductance	100 mH
Grid voltage	400 V
Rated frequency	50 Hz
Switching frequency	2000 Hz
Base power	1 kW
Base voltage: V_{L-L}	400 V

and reactive powers can be changed by regulating the *q* and *d* components of the filter capacitor voltage, respectively [19]. Then, it can be equivalently seen as a voltage source by the filter capacitor. The schematic diagram of the proposed system is shown in Fig. 7.

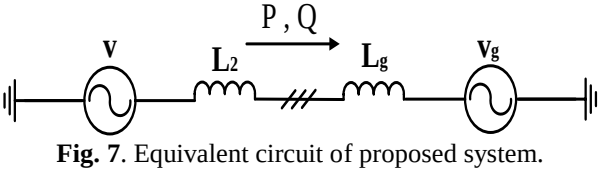

Fig. 7. Equivalent circuit of proposed system.

Assuming that the grid voltage initial phase is zero, the active and reactive powers transmitted from the inverter to the grid are given by:

$$P = \frac{3V_g V \sin\delta}{X_{eq}} = \frac{3V_g V \sin\delta}{\omega_0 (L_2 + L_g)} \quad (20)$$

$$Q = \frac{3V_g V \cos\delta}{X_{eq}} = \frac{3V_g V \cos\delta}{\omega_0 (L_2 + L_g)} \quad (21)$$

Where, V_g is the Root Mean Square (RMS) value of the grid phase voltage, V is the RMS value of filter capacitor phase voltage, δ is the leading angle of the capacitor voltage with regard to the grid voltage and ω_0 is the angular frequency of the grid voltage.

It should be noted that regulating the *q* channel will control the active power transmitted to the grid, similar to the *d* channel with the reactive power.

5. SIMULATION RESULTS

This section deals with simulation of Fig. 1 in MATLAB/Simulink environment. The system parameters are presented in Table 1. The load is Z=50+j31.416 and the MT outputs are on per unit.

For hybrid operations, at first a load equal to 0.5Z is supplied to MTG and then, it is connected to the grid at t=10s. The stand-alone mode power is about twice as large as the grid-connected mode's power, since in the latter, power-sharing with grid reduces the MTG output power. Three-phase voltages remain constant at 400 V with low THD and current's alteration.

The MTG active power is shown in Fig. 8. Before grid connection, the MTG meets the demands independently, but after that, power sharing occurs and more than half of the power is supplied by the grid.

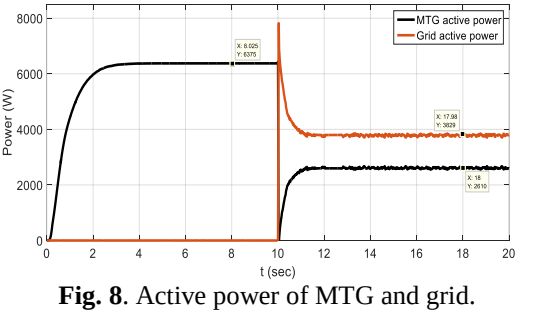

Fig. 8. Active power of MTG and grid.

Fig. 9 displays the three-phase load voltages which have 400 V amplitude and 50 Hz frequency. The switch between two operational modes creates a little transient waveform.

Fig. 10 shows the grid-side and MTG-side three-phase currents. The MTG current is 13 A for stand-alone mode which increases to 35 A for the grid-connected mode. According to Fig. 10 (b), the grid-side current is initially zero which grows up to 30 A.

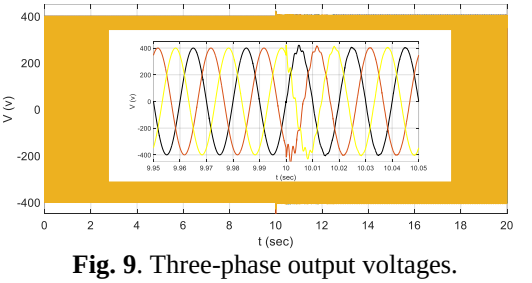

Fig. 9. Three-phase output voltages.

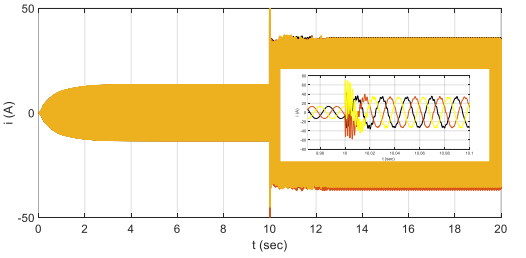

(a)

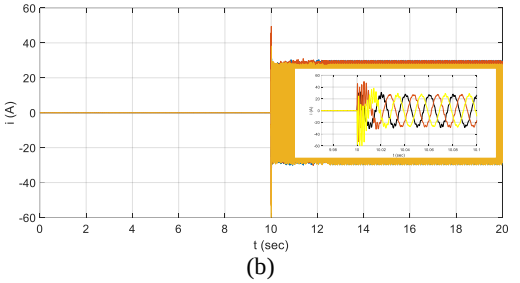

(b)

Fig. 10. Three-phase currents: (a) MTG-side (b) grid-side.

The fuel demand signal and MTG speed are shown in Fig. 11 and Fig. 12, respectively. By connecting the MTG to the grid, the fuel level is reduced and the speed reaches steady-state at a higher level, because the MTG output power has diminished in the presence of the grid.

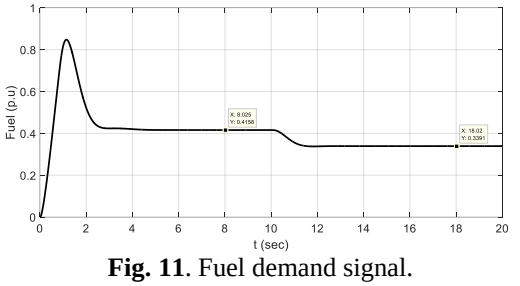

Fig. 11. Fuel demand signal.

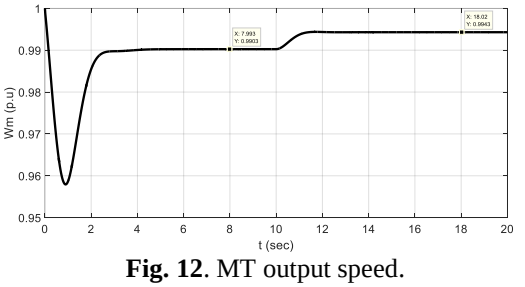

Fig. 12. MT output speed.

Fig. 13 and Fig. 14 show the electromagnetic torque and output power of the MTG, respectively. Since the MTG generates less power in the grid-connected mode, the PMSG torque and power drop similar to other inherent parameters.

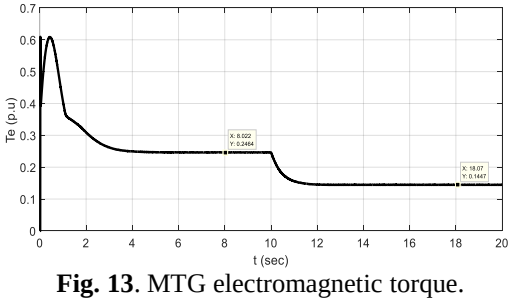

Fig. 13. MTG electromagnetic torque.

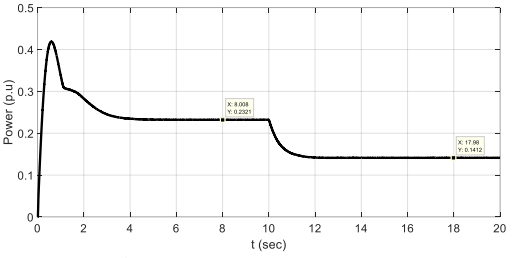

Fig. 14. MTG output power.

The results confirm the desirable performance of the MT in two different operating modes. In spite of the fast transit state and mode change, the MT adjusts its production with the grid.

6. CONCLUSION

Recently, MTGs are used as highly efficient and flexible sources in many applications such as emergency power. The MTG must possess quick performance to supply demands, which requires appropriate control methods.

In this paper, hybrid operation of the MTG was considered and a novel strategy was applied for the grid-connected state. Robust control in stand-alone mode along with power-voltage control in grid-connected mode help MTG to follow the demands properly. Two control methods were used instead of traditional strategies. The simulation results indicated MTG's fast response to changes in the situation and appropriate power sharing between the MT and the grid.

REFERENCES

[1] P. Breeze, Microturbines. In: Breeze P, editor. "Gas-Turbine Power Generation", *4 Netherland: Elsevier Science & Technology Books*, pp. 77-82, 2016.

[2] M. S. Ismail, M. Moghavvemi, T. Mahlia, **"Current Utilization of Microturbines as a Part of a Hybrid System in Distributed Generation Technology",** *Renewable and Sustainable Energy Reviews 2013*; 21, pp. 142-152, 2013.

[3] P. Asgharian, R. Noroozian, "Microturbine Generation Power Systems", In: Gharehpetian GB, Mousavi Agah SM, editors. Distributed Generation Systems: Design, Operation and Grid Integration. Netherland: Butterworth-Heinemann, Elsevier Science & Technology Books, pp. 149-219, 2017.

[4] Nayak SK, Gaonkar DN. **"Modeling and Performance Analysis of Microturbine Generation System in Grid Connected/Islanding Operation",** *International Journal of Renewable Energy Research* 2012, 2, pp. 750-757, 2012.

[5] M. Ranjbar, S. Mohaghegh, M. Salehifar, H. Ebrahimirad, A. Ghaleh **"Power Electronic Interface in a 70 kW Microturbine-Based Distributed Generation",** In: *IEEE 2nd Power Electronics, Drive Systems and Technologies Conference*; 16-17, Tehran, Iran: IEEE. pp. 111-116, 2011.

[6] G. Saravanan, I. Gnanambal, **"Design and Efficient Controller for Micro Turbine System",** *Circuits and Systems*, 7, pp. 1224-1232, 2016.

[7] S. Sarajian, **"Design and Control of Grid Interfaced Voltage Source Inverter with Output LCL Filter",** *International Journal of Electronics Communications and Electrical Engineering*, Vol. 4, pp. 26–40, 2014.

[8] A. K. Saha, S. Chowdhury, S. P. Chowdhury, P. A. Crossley **"Modeling and Performance Analysis of a Microturbine as a Distributed Energy Resource",** *IEEE T ENERGY CONVER 2009*; 24, pp. 529-538, 2009.

[9] P. Asgharian, R. Noroozian **"Modeling and Simulation of Microturbine Generation System for Simultaneous Grid-Connected/Islanding Operation",** *In: IEEE 24th Iranian Conference on Electrical Engineering (ICEE); 10-12 May 2016; Shiraz, Iran: IEEE*. pp. 1528-1533, 2016.

[10] G. Shankar, V. Mukherjee, **"Load-following Performance Analysis of a Microturbine for Islanded and Grid Connected Operation",** INT J ELEC POWER 4, 55, pp. 704-713, 2014.

[11] P. Asgharian. R. Noroozian, **"Dynamic Modeling of a Microturbine Generation System for Islanding Operation based on Model Predictive Control",** In: *31st international Power System Conference (PSC);* 24-26 Tehran, Iran, 2016.

[12] H. Keshtkar, J. Solanki, S. K. Solanki, **"Dynamic Modeling, Control and Stability Analysis of Microturbine in a Microgrid",** *IEEE PES T&D Conference and Exposition, Chicago,* USA, 2014.

[13] Mousavi GSM. An autonomous hybrid energy system of wind/tidal/microturbine/battery storage. INT J ELEC POWER 2012; 43: 1144-1154.

[14] G. Comodi, M. Renzi, L. Cioccolanti, F. Caresana, L. Pelagalli, **"Hybrid System with Micro Gas Turbine and PV (Photovoltaic) Plant: Guidelines for Sizing and Management Strategies**", *ENERGY 2015*; 89: pp. 226-235, 2015.

[15] D. P. Bakalis, A. G. Stamatis, **"Incorporating Available Micro Gas Turbines and Fuel Cell: Matching Considerations and Performance Evaluation",** *APPL ENERG 2013*; 103, pp. 607-617, 2013.

[16] S. Baudoin, L. Vechiu, H. Camblong, J. Vinassa, L. Barelli, **"Sizing and Cntrol of a Solid Oxide Fuel Cell/Gas Microturbine Hybrid Power System using a Unique Inverter for Rural Microgrid Integration",** *APPL ENERG 2016*; 176, pp. 272-281, 2016.

[17] P. Krause, **"Oleg Wasynczuk, Scott Sudhoff, Steven Pekarek, Analysis of Electric Machinery and Drive Systems",** *Wiley-IEEE Press*, 2013.

[18] M. R. Miveh, M. F. Rahmat, A. A. Ghadimi, M. W. Mustafa. **"Control Techniques for Three-Phase Four-Leg Voltage Source Inverters in Autonomous Microgrids: A Review",** *Renew Sust Energ Rev 2016*; 54: pp. 1592–1610, 2016.

[19] Sh. Sang, N. Gao, X. Cai, and R. Li. **"A Novel Power-Voltage Control Strategy for the Grid-Tied Inverter to Raise the Rated Power Injection Level in a Weak Grid",** *IEEE Journal of Emerging and Selected Topics in Power Electronics*, Issue: 99, 2017.